

Magnetic properties of disordered CoCu alloys : A first principles approach

Subhradip Ghosh¹ and Abhijit Mookerjee
*S.N. Bose National Centre for Basic Sciences,
JD Block, Sector 3, Salt Lake City, Calcutta 700091, India.*

Crystalline $\text{Co}_x\text{Cu}_{1-x}$ alloys show interesting magnetic behavior over the entire concentration regime. We here present a fully self-consistent first principles electronic structure studies of the electronic structure and magnetic properties of the system. We present results for the variation of density of states, magnetic moment, spin susceptibility and Curie temperature.

PACS no : 71.20, 71.20c

Keywords : Magnetism, Alloys, Augmented Space Recursion

I. INTRODUCTION

CoCu alloys have been extensively studied experimentally. Earlier investigations, particularly those of the magnetic properties, include high-temperature magnetic moment for 40- 85% Cu rich Co-Cu solid solutions [1] and variation of magnetic moments for Co rich alloys at room temperature [2,3]. Recently, the focus of attention has been on giant magneto-resistance (GMR) studies. Several experimental groups have been carrying studies of GMR in this system. Most remarkable works include investigation of GMR in bulk $\text{Co}_x\text{Cu}_{1-x}$ alloys for $x = 0.05-0.2$ [4,5], in heterogeneous thin film CoCu alloys [6,7] and in as-grown, epitaxial Co-Cu alloy layers [8]. Other magnetic studies on this system include magnetic anisotropy of Co on Cu(110) [9] and of Co-Cu ultra thin films [10]. An altogether different type of work by Childress and Chien [11] is, to our knowledge, the only one of its kind which involved low-temperature magnetic studies of $\text{Co}_x\text{Cu}_{1-x}$ alloys. This work is worth mentioning because it revealed very interesting features of the magnetic phases over the entire concentration range from $x = 0$ to $x = 0.8$. It indicated a low-temperature spin glass phase upto $x = 0.23$; a low-temperature re-entrant spin-glass or mixed phase, stable in the range $0.24 < x < 0.40$ and the normal low-temperature long-ranged random ferromagnetic phase stable beyond $x = 0.4$. Mandal and Ghatak [12] have reported calculations on the periodic Anderson model for a binary alloy, working within the Hartree-Fock, coupled with the Virtual Crystal Approximation (VCA). They have been able to produce some of the features observed experimentally. The model used by these authors have many empirical fitted parameters. The existence of a spin-glass and, at higher concentrations, a re-entrant mixed phase has been known from several mean-field approaches [13,14]. To our knowledge, the system has never been investigated from a first-principles electronic structure point of view. The aim of this com-

munication is to present such a calculation of magnetic properties of the fcc, ferromagnetic phase of $\text{Co}_x\text{Cu}_{1-x}$ alloys in the concentration range from 40% to 80% of Co. We have used the fully self-consistent, tight-binding linearized muffin-tin orbitals augmented space recursion (TB-LMTO-ASR) technique as the basis of our calculations. We have restricted ourselves to the ferromagnetic phase only leaving the spin-glass and mixed phases for a later study. Our studies involved calculation of magnetic moments, Curie temperatures and the spin susceptibilities.

II. THEORETICAL DETAILS

A. The magnetic phases

Description of magnetic phases within the local spin density approximation (LSDA) involves the study of the evolution of local magnetic moments in the vicinity of ion cores because of the distribution of the valence electron charge. Each lattice site in the face centered cubic structure is occupied by an ion core : in our case randomly by either Co or Cu. We shall associate a cell or a sphere with each ion core and assume that the charge contained in the sphere belongs to that ion core alone. Ideally such cells or spheres should not overlap. In the traditional Kohn-Korringa-Rostocker (KKR) method this is certainly so. However, in the atomic sphere approximation (ASA) which we shall use in our TB-LMTO version, this division of space is to a certain extent arbitrary. Within these cells the valence electrons carrying spin σ sees a binary random spin-dependent potential $V_\sigma^\lambda(\underline{r})$, where $\lambda = \text{Co or Cu}$ and $\sigma = \uparrow \text{ or } \downarrow$.

The charge density within the cells can be obtained from the partially averaged Green functions :

$$\begin{aligned} \tilde{\rho}_\sigma(r) = & -(1/\pi)\Im m \sum_L \int_{-\infty}^{E_F} [x \ll G_{LL}^{Co,\sigma}(r,r,E) \gg \\ & + (1-x) \ll G_{LL}^{Cu,\sigma}(r,r,E) \gg] dE \end{aligned} \quad (1)$$

where $\ll G_{LL}^{Co,\sigma}(r,r,E) \gg$ and $\ll G_{LL}^{Cu,\sigma}(r,r,E) \gg$ are partially averaged Green functions with the site r occupied by a Co or Cu ion core potential corresponding to spin σ .

For the random ferromagnetic phase we proceed as follows : we consider all cells to be identical in that they all carry identical average charge densities. We shall borrow the notation of Andersen *etal* [15] to write functions like $\tilde{f}(r_R)$ which are equal to $f(r)$ when r lies in the atomic sphere labelled by R and is zero outside. The ferromagnetic charge densities are defined as :

$$\begin{aligned} \rho_1(r) &= \sum_R \tilde{\rho}_\uparrow(r_R) \\ \rho_2(r) &= \sum_R \tilde{\rho}_\downarrow(r_R) \end{aligned}$$

The magnetic moment per cell (atom) is then defined by :

$$\begin{aligned} m &= (1/N) \int d^3r [\rho_1(r) - \rho_2(r)] \\ &= (1/N) \sum_R \int_{r \leq S} d^3r [\tilde{\rho}_\uparrow(r_R) - \tilde{\rho}_\downarrow(r_R)] \\ &= (1/N) \sum_R \int_{r \leq S} d^3r m_R(r_R) \end{aligned}$$

Since all cells are identical, the above calculation need be done only in one typical cell. Within the TB-LMTO-ASA the cells are replaced by inflated atomic spheres and the remaining interstitial is neglected. The problem is then one of a binary alloy with an almost non-magnetic charge density due to the Cu ion cores and a magnetic one due to the Co ones. The averaging is done over configurations of the random alloy.

B. The configuration averaging and TBLMTO-ASR

For random alloys we extract physical properties using configuration averaging which means that the physical quantities involved are the configuration averaged quantities. A powerful technique of carrying out this averaging is the augmented space recursion [16]. The method allows us to go well beyond the traditional single site coherent potential approximations and has been applied successfully to a wide variety of systems [17–20]. The convergence of the ASR has been established recently [21], so that any approximation we impose on the recursion is controlled by tolerance limits preset by us. ASR coupled with TB-LMTO-ASA has been proved to be a very powerful technique in predicting material properties.

The TB-LMTO-ASR has been described in great detail earlier [16–19,22]. We shall refer the reader to the referenced monograph for technical details. Here we quote only the main results.

Our starting point is the TB-LMTO Hamiltonian in atomic sphere approximation (ASA) :

$$H^{(\gamma)} = E_\nu + hI$$

where, $h = C - E_\nu + \Delta^{1/2}S\Delta^{1/2}$.

C , and Δ are diagonal matrices in angular momentum space and are the potential parameters of the TB-LMTO technique and S is the structure matrix which is sparse in the most tight-binding representation.

Let us now look at the transformation of the Hamiltonian in the full augmented space when the potential parameters have homogeneous binary random distributions. Such random variation may be described by random site occupation variables n_R which take values 1 or 0 according to whether the site R is occupied by an A-type or B-type of atom and have probability densities

$$p(n_R) = x \delta(n_R - 1) + (1 - x) \delta(n_R)$$

The details of construction of the augmented space and the effective Hamiltonian on it has been described in detail in our earlier communications [18,23,26]. We shall quote here only the final result and refer the readers to the referenced works. The trick involves first in replacing each random parameter P in the Hamiltonian by expressions of the type :

$$P_A n_R + P_B (1 - n_R) = P_B + (P_A - P_B) n_R \quad (2)$$

and then replacing each factor n_R by an operator \mathcal{M}_R which acts on the configuration space of n_R . For a binary distribution of n_R the rank of this space is two. We shall construct a basis in this space which we shall designate as $\{|\uparrow\rangle, |\downarrow\rangle\}$. For the binary distribution this operator is

$$\mathcal{M}_R = x\mathcal{P}_\uparrow^R + (1-x)\mathcal{P}_\downarrow^R + \sqrt{x(1-x)} \{\mathcal{T}_{\uparrow\downarrow}^R + \mathcal{T}_{\downarrow\uparrow}^R\}$$

and the above equation becomes :

$$\begin{aligned} &= \mathbf{A}(P)\mathcal{I} + \mathbf{B}(P)\mathcal{P}_\downarrow^R + \mathbf{F}(P) \{\mathcal{T}_{\uparrow\downarrow}^R + \mathcal{T}_{\downarrow\uparrow}^R\} \\ &= \hat{P} \end{aligned}$$

where

$$\begin{aligned} \mathbf{A}(P) &= x P_A + (1 - x) P_B \\ \mathbf{B}(P) &= (1 - 2x) (P_A - P_B) \\ \mathbf{F}(P) &= \sqrt{x(1 - x)} (P_A - P_B) \end{aligned}$$

We now proceed as follows :

$$\begin{aligned} (E - H)^{-1} &= (E - C - \Delta^{1/2}S\Delta^{1/2})^{-1} \\ &= \Delta^{-1/2} \left[\frac{E - C}{\Delta} - S \right]^{-1} \Delta^{-1/2} \end{aligned} \quad (3)$$

All factors except S have binary random distributions. Using the procedure described above we may now convert the above equation into augmented space. The augmented space theorem gives [23]

$$\ll G_{RL,RL}(E) \gg = \langle R, L, \{\emptyset\} | (E\hat{I} - \hat{H})^{-1} | R, L, \{\emptyset\} \rangle$$

First note that :

$$\begin{aligned} \tilde{\Delta}^{-1/2} | R, L, \{\emptyset\} \rangle &= \mathbf{A}(\Delta^{-1/2}) | R, L, \{\emptyset\} \rangle \\ &+ \mathbf{F}(\Delta^{1/2}) | R, L, \{R\} \rangle = | 1 \rangle \end{aligned} \quad (4)$$

and if we define $[\mathbf{A}(1/\Delta)]^{1/2} | 1 \rangle$ as $| 1 \rangle$, then this latter ket is normalized. A little algebra then gives :

$$\ll G_{RL,RL}(E) \gg = \langle 1 | [E - \hat{A} + \hat{B} + \hat{F} - \hat{S}]^{-1} | 1 \rangle \quad (5)$$

where

$$\begin{aligned} \hat{A} &= \{ \mathbf{A}(C/\Delta) / \mathbf{A}(1/\Delta) \} \mathcal{I} \otimes \mathcal{I} \otimes \mathcal{I} \\ \hat{B} &= \{ \mathbf{B}((E-C)/\Delta) / \mathbf{A}(1/\Delta) \} \sum_{RL} \mathcal{P}_R \otimes \mathcal{P}_L \otimes \mathcal{P}_\downarrow^R \\ \hat{F} &= \{ \mathbf{F}((E-C)/\Delta) / \mathbf{A}(1/\Delta) \} \sum_{RL} \mathcal{P}_R \otimes \mathcal{P}_L \\ &\otimes \{ \mathcal{T}_{\uparrow\downarrow}^R + \mathcal{T}_{\downarrow\uparrow}^R \} \\ \hat{S} &= \sum_{RL} \sum_{R'L'} \left\{ \mathbf{A}(1/\Delta)^{-1/2} \right\} S_{RL,R'L'} \left\{ \mathbf{A}(1/\Delta)^{1/2} \right\} \mathcal{T}_{RR'} \\ &\otimes \mathcal{T}_{LL'} \otimes \mathcal{I} \end{aligned} \quad (6)$$

and $\hat{J} = \hat{J}_A + \hat{J}_B + \hat{J}_F$ where the operators on the right hand side of these equations are given by

$$\begin{aligned} \hat{J}_A &= \{ \mathbf{A}((C-E_\nu)/\Delta) / \mathbf{A}(1/\Delta) \} \mathcal{I} \otimes \mathcal{I} \otimes \mathcal{I} \\ \hat{J}_B &= \{ \mathbf{B}((C-E_\nu)/\Delta) / \mathbf{A}(1/\Delta) \} \sum_{RL} \mathcal{P}_R \otimes \mathcal{P}_L \otimes \mathcal{P}_\downarrow^R \\ \hat{J}_F &= \{ \mathbf{F}((C-E_\nu)/\Delta) / \mathbf{A}(1/\Delta) \} \sum_{RL} \mathcal{P}_R \otimes \mathcal{P}_L \\ &\otimes \{ \mathcal{T}_{\uparrow\downarrow}^R + \mathcal{T}_{\downarrow\uparrow}^R \} \end{aligned}$$

This form is suitable for recursion. We start the recursion with the *state* $| 1 \rangle$ which is a mixture of the configurations $\{\emptyset\}$ and $\{R\}$ and carry out recursion as usual.

The initial TB-LMTO potential parameters are obtained from suitable guess potentials as described in the article by Andersen *etal* [15]. In subsequent iterations the potentials parameters are obtained from the solution of the Kohn-Sham equation

$$\left\{ -\frac{\hbar^2}{2m} \nabla^2 + V^{\nu\sigma} - E \right\} \phi_\sigma^\nu(r_R, E) = 0 \quad (7)$$

where,

$$V^{\nu\sigma}(r_R) = V_{core}^{\nu\sigma}(r_R) + V_{har}^{\nu\sigma}(r_R) + V_{xc}^{\nu\sigma}(r_R) + V_{mad} \quad (8)$$

here ν refers to the species of atom sitting at R and σ the spin component. The electronic position within the atomic sphere centered at R is given by $r_R = r - R$. The core potentials are obtained from atomic calculations and are available for most atoms. The treatment of the Madelung potential in a random alloy has always raised problems. We adopt a procedure suggested by Drchal *etal* [24] and regularly used in CPA calculations within the TB-LMTO. We choose the atomic sphere radii of the components in such a way that they preserve the total volume on the average and the individual atomic spheres are almost neutral. This ensures that total charge is conserved, but each atomic sphere carries no excess charge. However, we are careful that such a choice does not violate the overlap criterion of Andersen and Jepsen [15]. In the ASR-LSDA self-consistency loop, charge transfer takes place between these spheres ; however, at the end of the self-consistency iterations, the spheres are approximately neutral and hence do not contribute to a Madelung energy. This prescription is to an extent *ad hoc*, and there is no guarantee in general that we will be able to find such atomic sphere radii. However, the procedure has proved rather successful in many earlier CPA [24] and ASR [25] calculations on magnetic alloys and we shall adopt it here. As in the CPA calculations we iterate until the total energy and moments of the charge density converge. In this sense our calculations are self-consistent in the LSDA sense.

C. Curie temperature

We have estimated the Curie temperature by two different methods-Bragg Williams approximation and Mohn-Wolfarth model [28]. Both the procedures are described below:

1. Bragg-Williams approximation:

The estimates of the Curie temperature were obtained from the magnetic pair energies [26] The pair energies are defined as follows : At two sites labeled r and r' in a completely random paramagnetic background, we replace the potential by that of either the up-spin ferromagnetic Co or the down-spin one. The Green function of this system we shall denote by : $G_{LL}^{Co,\sigma\sigma'}(r, r, E)$, σ being the spin type at the site r (either \uparrow or \downarrow) and σ' that at the site r' . The pair energy is defined as

$$\begin{aligned} E(R) &= \int_{-\infty}^{E_F} dE E [-(1/\pi) \Im m(G_{LL}^{Co,\uparrow\uparrow}(r, r, E) \\ &+ G_{LL}^{Co,\downarrow\downarrow}(r, r, E) - G_{LL}^{Co,\uparrow\downarrow}(r, r, E) \\ &- G_{LL}^{Co,\downarrow\uparrow}(r, r, E))] \end{aligned} \quad (9)$$

Here $R = r - r'$. We may either estimate the above directly, or to be more accurate we may use

the orbital peeling method of Burke [27]. The latter is an extension of the recursion method, where small differences of large energies (as in the definition of the pair energy) are obtained directly and accurately from the recursion continued fraction coefficients. Note that we have assumed that the dominant contribution to the pair energy comes from the band contribution and the rest approximately cancel out. The simplest Bragg-Williams estimate of the Curie temperature is

$$T_c = (1 - x)E(0)/\kappa_B$$

where

$E(0) = E(q = 0)$ and $E(q) = \sum_R \exp(iq \cdot R)E(R)$. Since the pair energy is short-ranged, a reasonable estimate of $E(0)$ is $\sum_{n < 3} Z_n E(R_n)$ where R_n is the n^{th} -nearest

neighbour vectors and Z_n is the number of n^{th} -nearest neighbours. The Bragg-Williams approach overestimates the Curie temperature and its generalization, the cluster variation method, yields better quantitative estimates. We have restricted ourselves to the Bragg-Williams nearest neighbour pair energy approximation.

2. Mohn-Wohlfarth model(MW):

In this model [28]the Curie temperature is given by:

$$\frac{T_C^2}{T_{SF}^2} + \frac{T_C}{T_{SF}} - 1 = 0$$

where,

T_C^S is the stoner Curie temperature given by,

$$I(E_F) \int_{-\infty}^{\infty} N(E) \left(\frac{\delta f}{\delta E} \right) dE = 1$$

$I(E_F)$ is the Stoner parameter obtained from the earlier calculations [29], $N(E)$ is the density of states per atom per spin [30] and f is the Fermi distribution function.

T_{SF} is the spin fluctuation temperature given by,

$$T_{SF} = \frac{m^2}{10k_B\chi_0}$$

χ_0 is the exchange enhanced spin susceptibility at equilibrium and m is the magnetic moment per atom.

χ_0 is calculated using the relation by Mohn [28] and Gersdorf [31]:

$$\chi_0^{-1} = \frac{1}{2\mu_B^2} \left(\frac{1}{2N^\uparrow(E_F)} + \frac{1}{2N^\downarrow(E_F)} - I \right)$$

I is the stoner parameter and $N^\uparrow(E_F)$ and $N^\downarrow(E_F)$ are the spin-up and spin-down density of states per atom.

III. COMPUTATIONAL DETAILS

For the calculation of the component projected averaged density of states of the ferromagnetic phase we have used a real space cluster of 400 atoms and an augmented space shell upto the sixth nearest neighbour from the starting state. Eight pairs of recursion coefficients were determined exactly and the continued fraction terminated by the analytic terminator due to Luchini and Nex [32]. In a paper Ghosh *etal* [21] have shown the convergence of the related integrated quantities, like the Fermi energy, the band energy, the magnetic moments and the charge densities, within the augmented space recursion. The convergence tests suggested by the authors were carried out to prescribed accuracies. We noted that at least eight pairs of recursion coefficients were necessary to provide Fermi energies and magnetic moments to required accuracies. We have reduced the computational burden of the recursion in the full augmented space by using the local symmetries of the augmented space to reduce the effective rank of the invariant subspace in which the recursion is confined [16] and using the seed recursion methodology [22] with fifteen energy seed points uniformly across the spectrum.

We have chosen the Wigner-Seitz radii of the two constituent atoms Co and Cu in such a way that the average volume occupied by the atoms is conserved. Within this constraint we have varied the radii so that the final configuration has neutral spheres. This eliminates the necessity to include the averaged Madelung Energy part in the total energy of the alloy. The definition and computation of the Madelung Energy in a random alloy had faced controversy in recent literature and to this date no satisfactory resolution of the problem exists. Simultaneously we have made sure that the sphere overlap remains within the 15% limit prescribed by Andersen.

The calculations have been made self-consistent in the LSDA sense, that is, at each stage the averaged charge densities are calculated from the augmented space recursion and the new potential is generated by the usual LSDA techniques. This self-consistency cycle was converged in both total energy and charge to errors of the order 10^{-5} . We have also minimized the total energy with respect to the lattice constant. The quoted results are those for the minimum configuration. No short ranged order due to chemical clustering has been taken into account in these calculations, nor any lattice distortions due to the size differences between the two constituents.

IV. RESULTS AND DISCUSSION

Figure 1(a) and 1(b) show the partial density of states at Co and at Cu sites respectively for various concentrations of Cu. It is evident from the figures that there is hardly any difference in the relative heights and shapes in the majority and minority spin bands at Cu site for various concentrations. This is reflected in the local magnetic moment shown in Figure 2 where Cu sites have a very small amount of induced moment. For the minority spin partial densities on Co, the structure below the Fermi level do not change much with the Co concentration. The peak at around 0.0 Ryd. grows with decreasing Co concentration. However, this structure is above Fermi level and does not contribute to the magnetic moment. For the majority spin partial densities on Co, the peak around -0.4 Ryd. doesn't change with concentration while the one around -0.3 Ryd. grows with concentration. The most remarkable change occurs in the peak around -0.2 Ryd. whose height reduces with the concentration and finally the peak around -0.3 Ryd. contributes more with increasing concentration. As a result, the partial magnetic moment on Co increases only slowly with concentration and the variation of average magnetic moment is linear as shown in Figure 2.

Figure 3 shows the variation of average magnetic moment in emu/gm unit and the agreement with experimental results [11] is pretty good qualitatively. Both CPA and ASR moments agree well too. But, the agreement with the results from model calculation [12] is far from being reasonable. Their calculations predict a monotonic fall of average magnetic moment and finally vanishing of magnetic moment around 40% of Co concentration. This has neither been observed in experiments [11] nor in our calculations with two widely used *ab-initio* methods. This discrepancy is due to the choice of technique in case of model calculations. They used Hartree-Fock and VCA for their calculations. Both the approximations have their own limitations in predicting properties of real materials. The very important electron-electron correlation effect is absent within the framework of Hartree-Fock approximation while in LSDA this effect has been incorporated. The limitation of VCA is that it has been proved to be successful only in cases of weak scattering alloys where each particle sees nearly the same average perturbation field. ASR on the other hand is a very powerful and accurate technique in the sense that it is an exact method involving no mean-field like approximation for configuration averaging. This is the reason for better agreement of our calculations with the experimental results.

Figure 4 shows the partial and average spin susceptibilities of the system. The partial susceptibility of Cu varies smoothly and finally becomes almost saturated while we find little oscillations in case of Co particularly in the range of 60%-80% of Co. This nature is reflected in the average susceptibility. This is basically due to oscillations

in the up density of states at Fermi energy at Co sites (See Table I). However, the oscillation in the Co as well as average susceptibilities are very small, eventually leading to saturation.

Figure 5 shows the variation of Curie temperature with Co concentration using Bragg Williams (BW) approximation and MW model. In BW approximation, the variation of Curie temperature is smooth though the values are overestimated. This is expected as BW approximation has a tendency to overestimate [33]. This overestimation is reduced using MW model but the qualitative agreement between the two methods is not obtained. In the concentration regime 40%-60% of Co, Curie temperature oscillates in MW model and beyond it qualitative agreement with BW calculations is achieved. This fluctuating behaviour obtained in MW calculations is due to the oscillations in Spin fluctuation temperature (See Table II) because Stoner Curie temperature has a systematic variation with Co concentration. This oscillation in spin fluctuation temperature can be explained as follows: for the concentration 40%-60% of Co the partial spin susceptibilities of both Co and Cu undergo variations which is reflected in the spin fluctuation temperature while for 60%-80% of Co the susceptibilities of both the components remain almost constant except for a small variation at around 80% of Co. That's why the spin fluctuation temperature and hence the Curie temperature follow the same trend as obtained in BW calculations for Co concentration beyond 60%. The Stoner Curie temperature (See Table II) is very high as expected because LSDA overestimates the binding. We have also tried to characterize the system for the concentration regime of our investigation following the prescription by Mohn and Wolfarth [28] which characterizes a system from the values of Curie temperature and spin fluctuation temperature. According to the prescription the quantity $t_c = \frac{T_c}{T_S}$ determines the agency playing the dominant role in finding out Curie temperature and hence the effect of spin fluctuations in determining the magnetic properties of the system. The systems with $t_c < 0.5$ are called *fluctuation* systems in which description of magnetism should involve spin fluctuation effects and systems with $t_c > 0.5$ are called *Stoner* systems in which single particle excitations play the dominant role. In our case, we see (See Table II) that for the entire range of concentrations t_c remains less than 0.5 which means that the description of magnetic properties should have the effect of spin fluctuations.

V. CONCLUSIONS

We have calculated for the first time, the electronic structure and magnetic properties of $\text{Co}_x\text{Cu}_{1-x}$ alloys using fully self-consistent first principles electronic structure technique and obtained results which agree reasonably well with the experimental results. This clearly shows that ASR coupled with TBLMTO is a powerful

technique in describing electronic structure and magnetic properties of binary alloys. Our results clearly show the flaws in the theoretical results based upon model calculations. Finally, this study clearly presents the fact that in CoCu alloy spin fluctuation effect is very much present in the ferromagnetic phase and a more accurate description of the magnetic properties of the system should involve this effect.

ACKNOWLEDGMENTS

AM and SG acknowledges useful discussions with Dr.Kalyan Mandal.

REFERENCES

-
- ¹ Corresponding author:e-mail :subhra@boson.bose.res.in
- [1] E. Kneller, *J. Appl. Phys.* **33** 1355(1963)
- [2] Bensus M.J .*etal*, *Physics Letters* **32A** 192(1970)
- [3] Crangle J., *Phil. Mag.* **46** 499(1955)
- [4] Yu R.H. *etal* *J.Phys.* **D28** 1770(1995)
- [5] Xiao John Q. *etal*, *Phys. Rev. Lett.* **68** 3749(1992)
- [6] Berkowitz A. E. *etal*, *J. Appl. Phys.* **73** 5320(1993)
- [7] Berkowitz A. E. *etal*, *Phys. Rev. Lett.* **68** 3745(1992)
- [8] Parkin S.S.P. *etal*, *Europhysics letters* **22** 455(1993)
- [9] Fassbender J. *et al*, *Phys. Rev.* **B57** 5870(1998)
- [10] Hope S. *et al*, *Phys. Rev.* **B57** 7454(1998)
- [11] Childress J.R. and Chien C.L., *Phys. Rev.* **B43** 8089(1991)
- [12] Mandal K. and Ghatak S.K., *Int.J.Mod.Phys.* **B9** 145(1995)
- [13] Mookerjee A., *Pramana* **14** 11(1980)
- [14] Gabay M. and Toulouse G., *Phys. Rev. Lett.* **47** 201(1981)
- [15] Andersen O K and Jepsen O , *Phys. Rev. Lett.* **53** 2571(1984)
- [16] Dasgupta I, Saha T and Mookerjee A , *J. Phys.* **C8** 1979(1996)
- [17] Dasgupta I, Saha T and Mookerjee A , *Phys. Rev.* **B51** 17724(1993)
- [18] Saha T, Dasgupta I and Mookerjee A , *J. Phys.* **C73413**(1995)
- [19] Sanyal B. and Mookerjee A., *Physics Letters* **246A** 151(1998)
- [20] Sanyal B.*et al*, *J. Phys.* **C11** 1833(1999)
- [21] Ghosh S, Das N and Mookerjee A , *J. Phys.* **C9** 10701(1997)
- [22] Ghosh S, Das N and Mookerjee A, *Int.J.Mod.Phys.* **B** (in press)
- [23] Saha T, Dasgupta I and Mookerjee A , *J. Phys.* **C6** L245 (1994)
- [24] Drchal V, Kudrnovský J and Weinberger P , *Phys. Rev.* **B50** 7903(1994)
- [25] Dasgupta I, Saha-Dasgupta T, Mookerjee A and Das G.P. , *J. Phys.* **C9** 3529(1997)
- [26] Mookerjee A 1998 *Electron correlations in atoms and solids* ed. Tripathi A N and Singh I (Phoenix Publishing House, New Delhi) pp 180-198
- [27] Burke N E , *Surf.Sci.* **58** 349(1976)
- [28] Mohn P. and Wohlfarth E.P., *J. Phys.* **F17** 2421(1987)
- [29] Janak J.F., *Phys. Rev.* **B16** 255(1977)
- [30] Gunnarson O., *J. Phys.* **F6** 587(1976)
- [31] Gersdorf R., *J.Phys.Radium* **23** 726(1962)
- [32] Luchini M U and Nex C M M , *J. Phys.* **C20** 3125(1987)
- [33] Ghosh S., Das N. and Mookerjee A., *J. Phys.* **C10** 11773(1998)

FIGURE CAPTIONS

Figure 1(a) shows the partial densities of states of Co at various Co concentrations. The concentrations are indicated in the inset. Dashed curves show the results for the minority and full curve the majority spin states. Fermi energies are indicated by vertical dashed lines with each figure.

Figure 1(b) shows the partial densities of states of Cu at various Co concentrations. The concentrations are indicated in the inset. Dashed curves show the results for the minority and full curve the majority spin states. Fermi energies are indicated by vertical dashed lines with each figure.

Figure 2 shows The partial magnetic moments on Co and Cu sites and the average magnetic moment as a function of Co concentration. The solid and dotted lines refer to the augmented space calculations while the squares, the crosses and diamonds to the CPA. All these values are in units of Bohr-magneton.

Figure 3 shows the average magnetization in emu/gm as a function of Co concentration at 0K obtained from the theoretical estimates. The solid line refers to the ASR calculations while the diamonds to CPA.

Figure 4 shows the average and partial spin susceptibilities($\frac{\chi}{2\mu_B^2}$) in Ryd⁻¹atom⁻¹ with Co concentration.

Figure 5 shows the Curie temperature as a function of Co concentration. The solid line corresponds to the results using BW approximation while the squares correspond to the results with MW model.

VI. TABLES

x_{co}	$N_{co}^{\uparrow}(E_F)$	$N_{co}^{\downarrow}(E_F)$	$N_{cu}^{\uparrow}(E_F)$	$N_{cu}^{\downarrow}(E_F)$	$\frac{\chi_{co}}{2\mu_B^2}$	$\frac{\chi_{cu}}{2\mu_B^2}$	$\frac{\chi_{av}}{2\mu_B^2}$
0.4	2.13	51.30	0.77	0.88	5.79	0.86	2.84
0.45	2.52	50.54	1.30	1.47	7.35	1.49	4.13
0.5	2.72	47.73	1.61	1.88	8.16	1.91	5.04
0.6	3.43	38.28	2.41	3.07	11.52	3.13	8.17
0.7	3.58	22.55	2.50	4.09	11.15	3.74	8.92
0.8	3.37	15.83	2.32	4.84	9.27	3.77	8.17

TABLE I. shows the density of states (both up and down) at fermi level for both the components and the partial and average susceptibilities with Co concentration

x_{co}	T_c^{BW}	T_{SF}	T_c^S	T_c^{MW}	t_c
0.4	1042	1169	7007	1138	0.16
0.45	1150	1089	7095	1064	0.15
0.5	1394	1134	7186	1107	0.16
0.6	1667	1016	7356	998	0.14
0.7	1911	1260	7530	1227	0.17
0.8	1983	1728	7709	1648	0.22

TABLE II. shows the values of BW Curie temperature(T_c^{BW}), MW Curie temperature(T_c^{MW}), spin fluctuation temperatures(T_{SF}) and Stoner Curie temperature(T_c^S) with Co concentration

Figure 1(a)

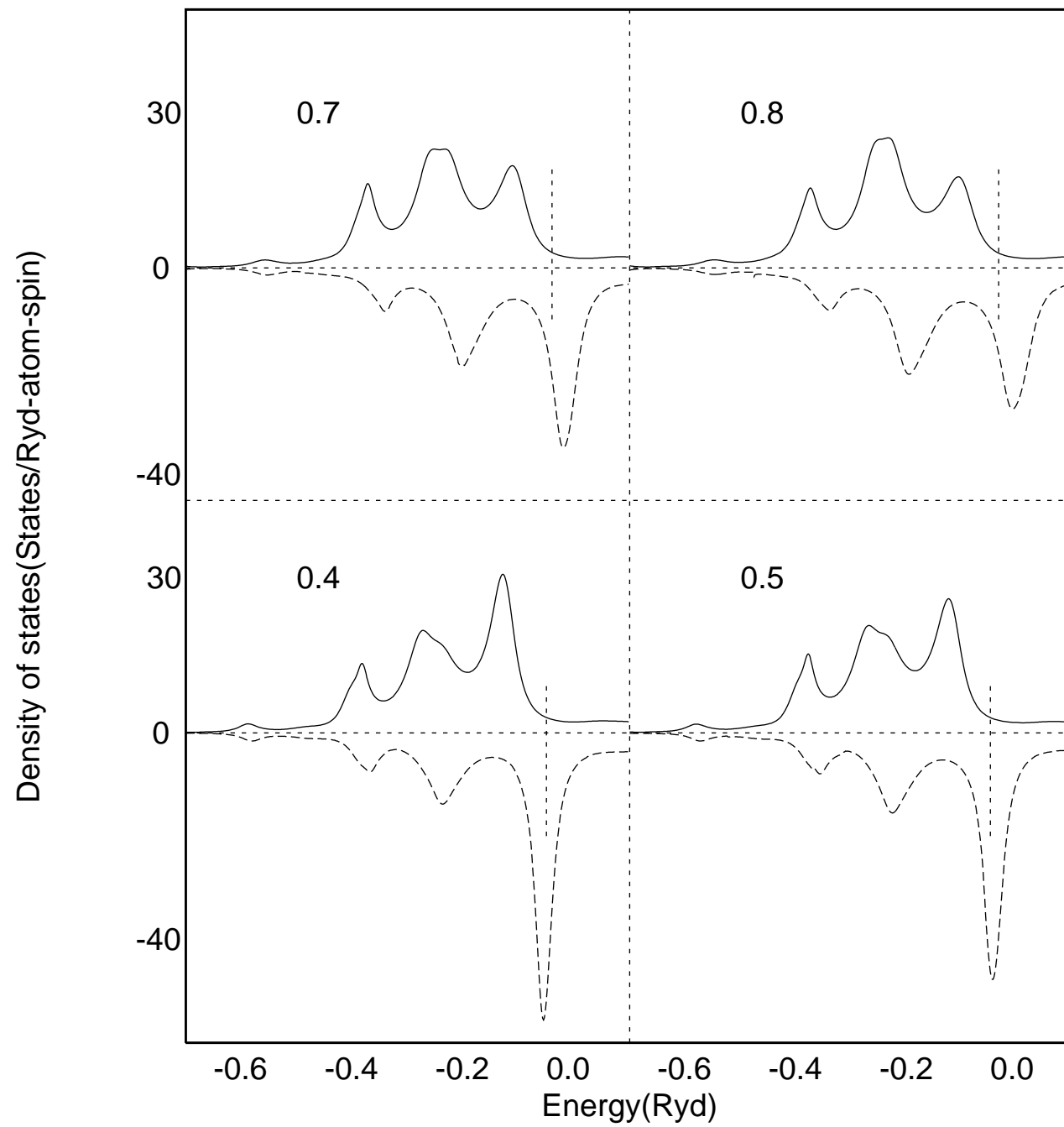


Figure 1(b)

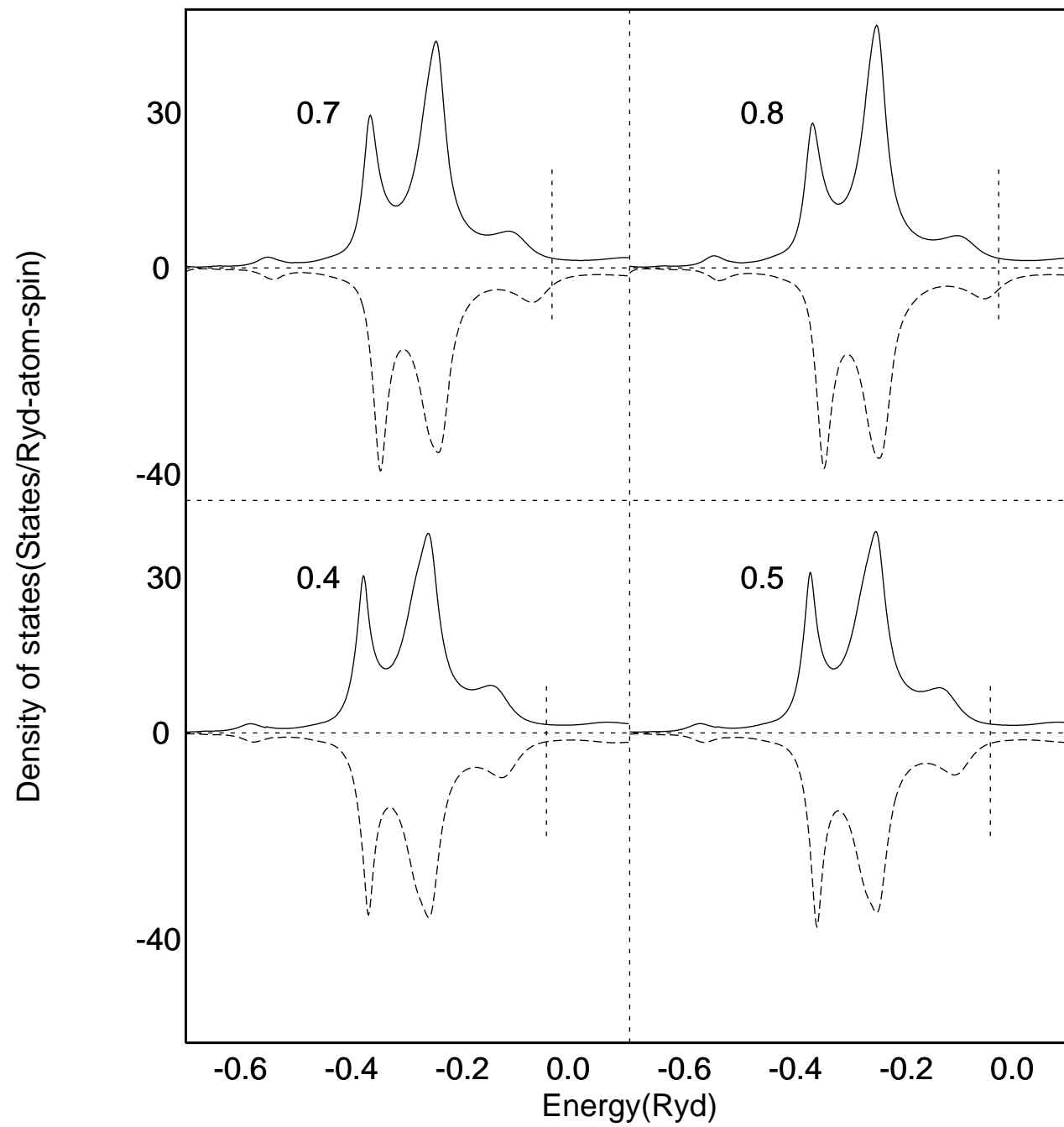


Figure 2

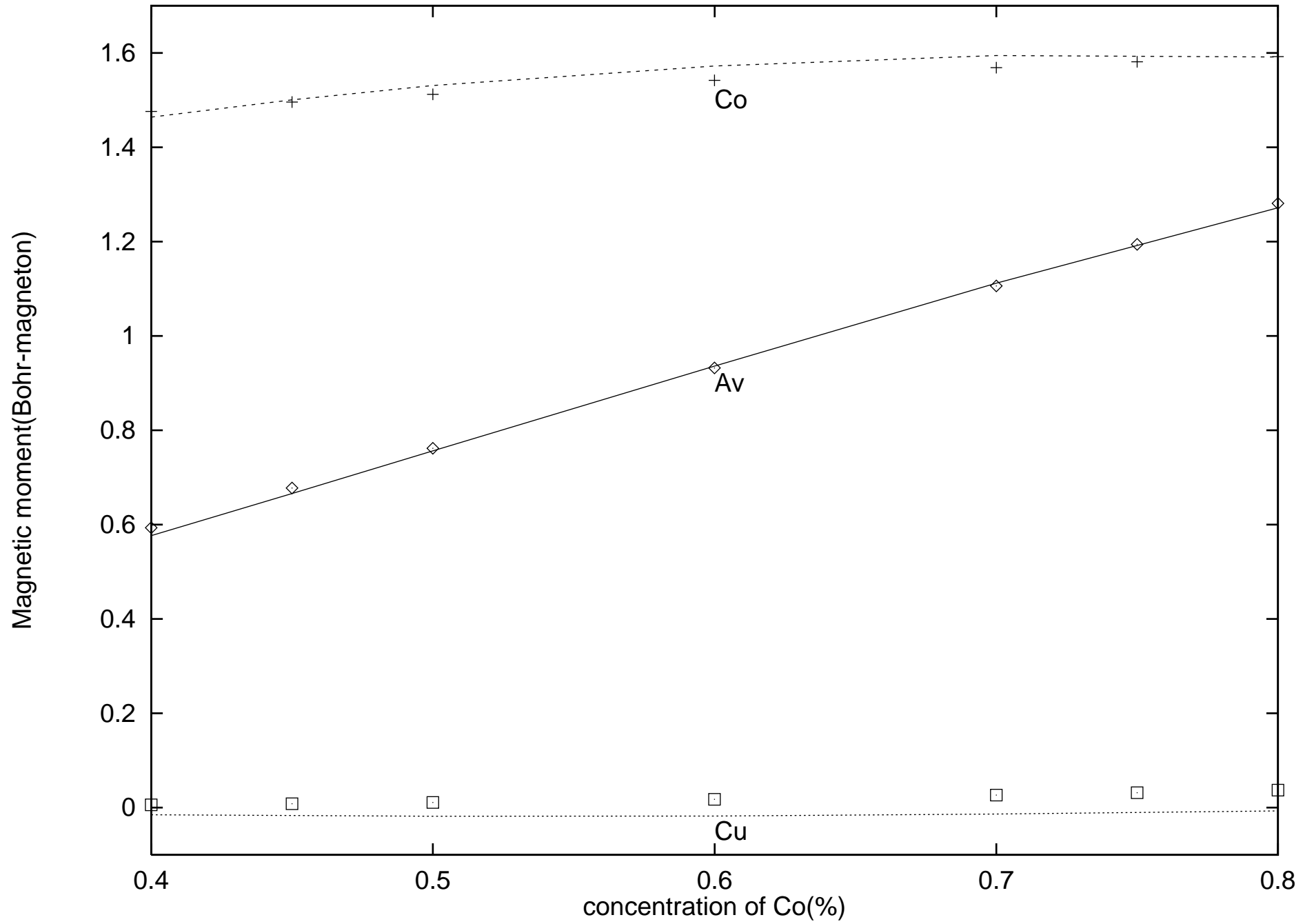


Figure 3

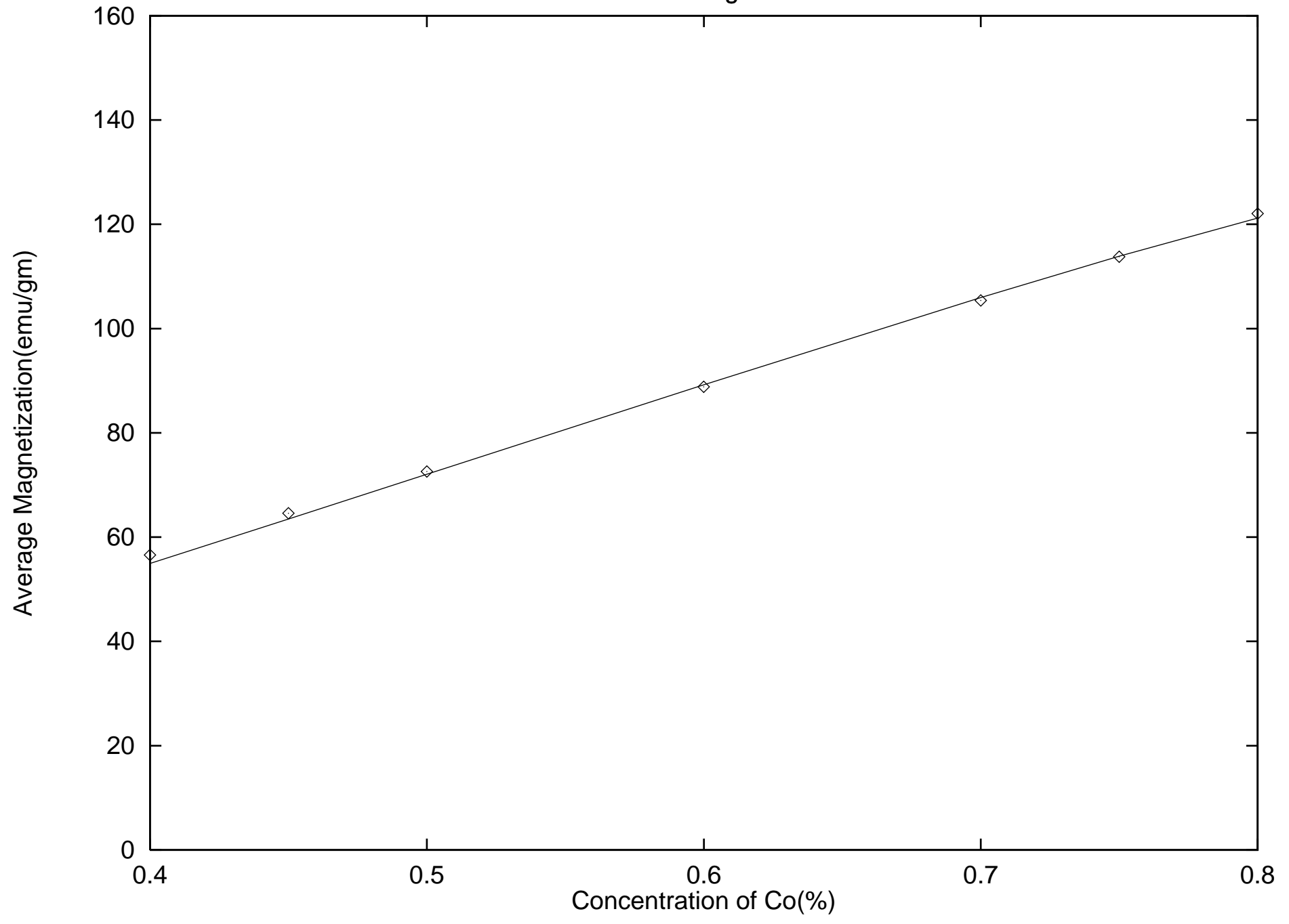


Figure 4

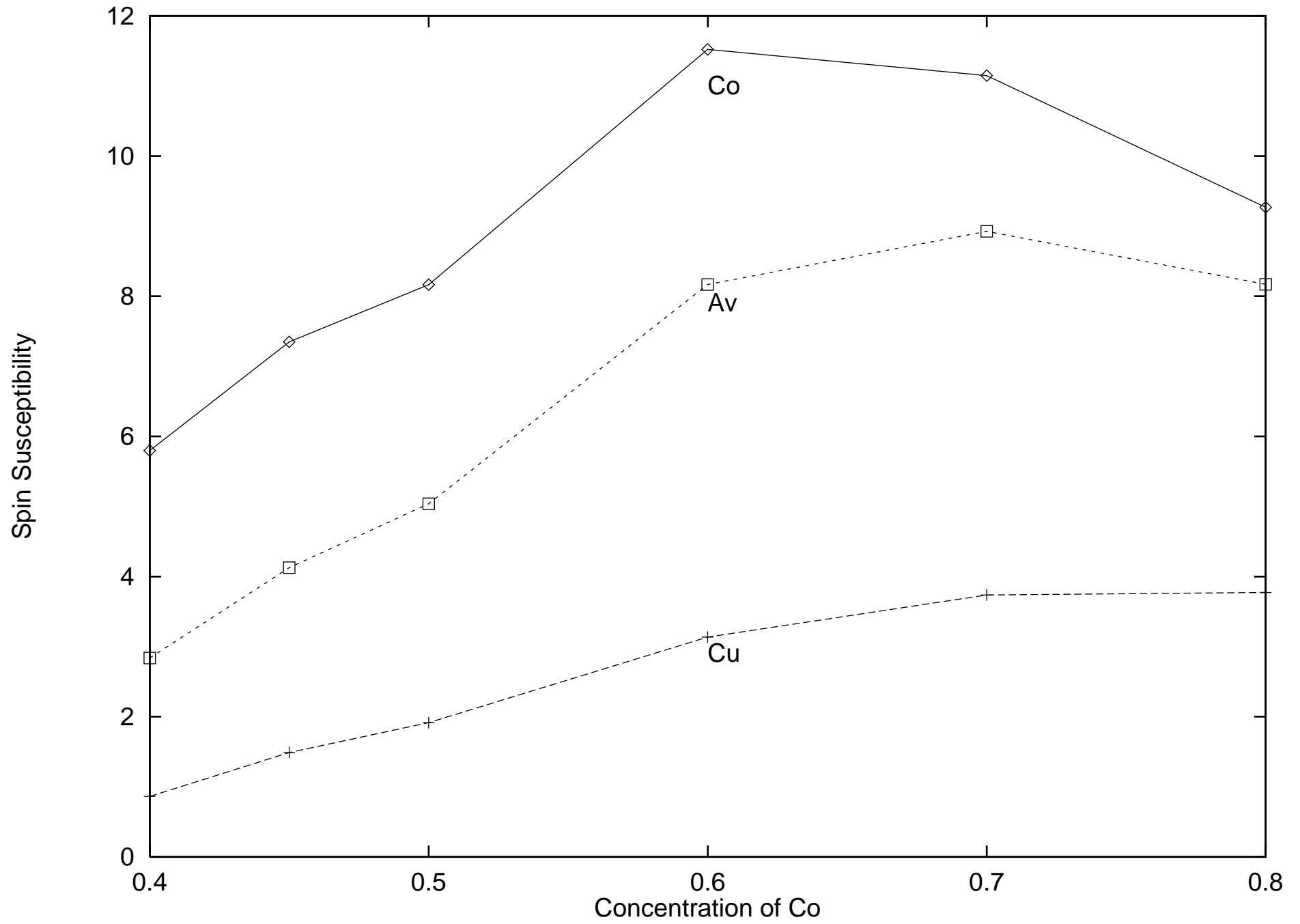


Figure 5

